1990

Numerical Analysis in the Flow Field of a Labyrinth Seal

K. W. Lee
Hanyang University

S. U. Lee
Hanyang University

C. H. Kim
Korea Institute of Science and Technology

T. H. Song
Korea Advanced Institute of Science and Technology

NUMERICAL ANALYSIS IN THE FLOW FIELD OF A LABYRINTH SEAL

Kwan Soo Lee[1], Sang Ug Lee[2], Chang Ho Kim[3], and Tae Ho Song[4]

[1] Associate Professor, Hanyang University, Seoul, Korea
[2] Graduate Research Assistant, Hanyang University, Seoul, Korea
[3] Senior Research Scientist, Korea Institute of Science and Technology, Seoul, Korea
[4] Assistant Professor, Korea Advanced Institute of Science and Technology, Taejon, Korea

ABSTRACT

This paper presents numerical analysis of the incompressible turbulent flow field in a single cavity of the stepped multi-cavity seal. The dimensionless bulk pressure drop for the cavity with and without groove has been investigated for four different Reynolds numbers and three different shaft rotating speeds. SIMPLER algorithm is applied to solve the Navier-Stokes equation and low - Reynolds number $k-\varepsilon$ equation which takes turbulent flow into account. For the constant Reynolds number, it was found that the dimensionless pressure drop is proportional to shaft speed. Especially, the increment is higher at the low Reynolds number and lower at the high Reynolds number. At no shaft rotation, the dimensionless bulk pressure drop is increased linearly with Reynolds number. When the axial speed is relatively high in comparision with the circumferential speed, the groove in a cavity creates high pressure drop giving low leakage.

NOMENCLATURE

c :annular clearance

C_1, C_2, C_μ : empirical turbulent model constants

k :turbulent kinetic energy

K : dimensionless turbulence kinetic energy , k/u_m^2

p : pressure

P : dimensionless pressure, $p/\rho u_m^2$

Re : Reynolds number, $2u_m c/\upsilon_l$

R_t : turbulent Reynolds number, $k/\upsilon_l\varepsilon$

U = (U, V, W) dimensionless time – mean velocity , u/u_m

u = (u,v,w) time-mean velocity (in x, r, θ direction)

u_m : axial entrance velocity

u′ : fluctuation velocity

x , r , θ : axial, radial and circumferential coordinates

X,R : dimensionless axial and circumferential coordinates, x/c and r/c,respectively

ε : energy dissipation rate

ε* : dimensionless energy dissipation rate, $\varepsilon/(u_m^3/c)$

υ^* : dimensionless dynamic viscosity , $\upsilon/u_m c$

υ_e : effective dynamic viscosity, $\upsilon_l+\upsilon_t$

υ_l : dynamic viscosity

υ_t : turbulent dynamic viscosity , $C_\mu k^2/\varepsilon$

ρ : density

σ_k : Prandtl-Schmidt number for k

σ_ε : Prandtl-Schmidt number for ε

1. INTRODUCTION

Most of rotational machines such as compressor, turbine, pump and engine are provided with seals to minimize fluid leakage due to pressure gradient. Proper optimization of the seal is very crucial for these high performance equipments. Since the leakage is a function of

various variables such as seal clearance, tooth thickness, cavity width, pressure difference and shaft speed within the cavity, the accurate prediction of effects of these parameters is very important for the optimization of the seal design.

Prior to 1970, most of researches in seal design had been focused on the leakage flow rate and pressure drop within the cavity using simplified analytical methods, from which it is not easy to get the detailed flow behavior in the labyrinth seal. Recent studies are emphasized to evaluate the detailed velocity and turbulence kinetic energy distribution within the seal. Stoff[1] has utilized the TEACH Code to demonstrate the turbulence flow field in a straight seal by solving the momentum equation with the standard k-ε turbulence model. Rhode[2] overcame the convergence problem involved in TEACH code with QUICK scheme and demonstrated the advantages of QUICK scheme over the other schemes based on the computation time. Demko[3] has shown that two recirculation zones are formed in the seal when the ratio of Taylor number to Reynold number is greater than unity and resulted in the high pressure drop and low leakage. However, this theory can not be directly applied to actual seal design because the usual shaft speed is lower than the above condition. Rhode[4] obtained two ideal geometries for the stepped seal from his study using the TEACH code with the QUICK scheme. Following a fabrication of the seal with these two geometries, he measured pressure distribution and the leakage for various pressure ratios and shaft speed with variation of the relative location of the rotor with respect to the stator, and obtained the flow coefficient for optimum seal using the Dodge's method [5]. Witting et al[6] obtained pressure distribution and heat transfer coefficient for various geometries and pressure ratios in the stepped seal. Rhode and Nail[7] expanded TEACH code to take the compressibility into account and analyzed the compressible turbulence flow field in a straight seal.

In this paper, the computer program is developed to predict the incompressible turbulent flow field in the stepped seal first, and then the pressure drops for the cavity with and without groove are evaluated for four different Reynolds numbers and three different shaft speeds.

2. FORMULATION OF THE PROBLEM

2.1 Model Selection and Assumptions

A schematic diagram of the physical model and coordinate system is given in Fig.1. Table 1 shows the dimensions of the model.

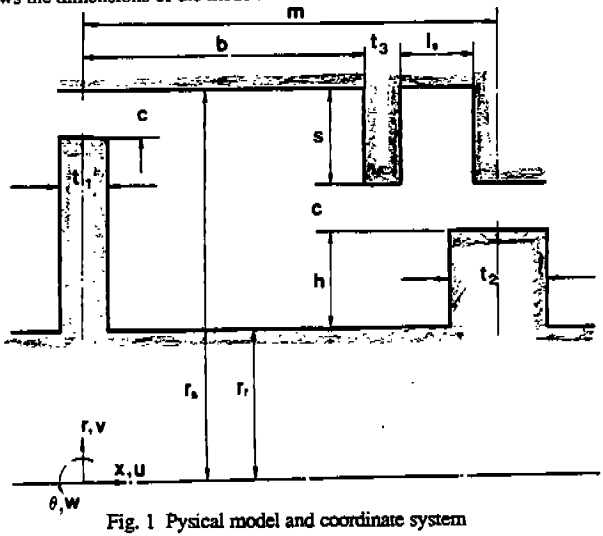

Fig. 1 Pysical model and coordinate system

Table 1 The cavity dimension (mm)

m	b	s	c	h	r_1
4.83	3.84	1.08	0.216	0.86	0.38
t_2	r_r	r_s	t_3	l_s	
1.05	90.944	93.1	0.21	0.59	

Following assumptions are applied to simplify the conservative equation to express the realistic physical characteristics of the flow field.

(a) The flow field is steady state, two dimension axisymmetrical, and turbulent.

(b) The flow is fully developed in θ-direction.

(c) The fluid is incompressible flow with constant density and viscosity.

2.2 Momentum Equation

The time averaged Navier-Stokes equation for the incompressible turbulent flow field can be expressed as follows with tensor notation :

$$\frac{\partial}{\partial x_j}(u_i u_j) = -\frac{1}{\rho}\frac{\partial p}{\partial x_i} + \frac{\partial}{\partial x_j}(\upsilon_l \frac{\partial u_i}{\partial x_j}) - \frac{\partial}{\partial x_j}(\overline{u'_i u'_j}) \qquad (1)$$

The expression $(\overline{u'_i u'_j})$ is the Reynolds stress term which requires turbulence modeling.

2.3 Turbulence Model

The standard k-ε turblence model is applied in the fully developed turbulent flow region. Very near the wall, the model is no longer valid because the viscosity increases and turbulent component decreases, hence low Reynolds number k-ε turbulence model or wall function may be taken. Since the geometry is too complex to be wall function modeled, following low Reynolds number k-ε turbulence model of Launder-Sharma[8] is selected.

$$\frac{Dk}{Dt} = \frac{\partial}{\partial x_j}(\upsilon_k \frac{\partial k}{\partial x_j}) + \upsilon_t \frac{\partial u_i}{\partial x_j}(\frac{\partial u_i}{\partial x_j} + \frac{\partial u_j}{\partial x_i}) - \varepsilon - 2\upsilon_l \left(\frac{\partial k^{1/2}}{\partial x_j}\right)^2 \qquad (2)$$

$$\frac{D\varepsilon}{Dt} = \frac{\partial}{\partial x_j}(\upsilon_\varepsilon \frac{\partial \varepsilon}{\partial x_j}) + C_1 \upsilon_t \frac{\varepsilon}{k}\frac{\partial u_i}{\partial x_j}(\frac{\partial u_i}{\partial x_j} + \frac{\partial u_j}{\partial x_i}) - \frac{C_2 \varepsilon^2}{k} + 2\upsilon_l \upsilon_t \left(\frac{\partial^2 u_i}{\partial u_j \partial u_k}\right)^2 \qquad (3)$$

where

$$\upsilon_k = \upsilon_l + \frac{\upsilon_t}{\sigma_k} \quad , \quad \upsilon_\varepsilon = \upsilon_l + \frac{\upsilon_t}{\sigma_\varepsilon}$$

The last term in equation (2) is artificially provided for easier computation and does not influence the numerical results. The last term in equation (3) is necessary for the value of ε at the wall to be zero.

2.4 Diffusion Coefficients and Source Term

The dimensionless turbulent flow equations in the cavity can be rewritten in the following standard form :

$$\frac{\partial}{\partial X_j}(U_j\phi) = -\frac{\partial P}{\partial X_i} + \frac{\partial}{\partial X_j}\left(\Gamma_\phi \frac{\partial \phi}{\partial X_j}\right) + S_\phi \qquad (4)$$

where , ϕ = one of the variables U, V, W, K and ε^*

Γ_ϕ = diffusion coefficient

S_ϕ = source per unit volume

The values of Γ_ϕ and S_ϕ are shown in Table 2. The equations and constants for the low Reynolds number k-ε turbulence model are given in Table 3.

Table 2 The form of the diffusion coefficient and source term in the general equation for ϕ

ϕ	Γ_ϕ	S_ϕ
U	υ_e^*	A
V	υ_e^*	$\frac{W^2}{R} - \upsilon_e^*\frac{V}{R^2} - \upsilon_i^*\frac{V}{R^2} + B$
W	υ_e^*	$-\frac{VW}{R} - \upsilon_e^*\frac{W}{R^2} - \frac{W}{R}\frac{\partial \upsilon_i^*}{\partial R}$
K	υ_e^*/σ_k	$G - \varepsilon^* - D$
ε^*	$\upsilon_e^*/\sigma_\varepsilon$	$(C_1 G\varepsilon^* - C_2\varepsilon^{*2})/K + E$

where

$$A = \frac{\partial}{\partial X}(\upsilon_i^*\frac{\partial U}{\partial X}) + \frac{1}{R}\frac{\partial}{\partial R}(\upsilon_i^* R\frac{\partial V}{\partial X})$$

$$B = \frac{\partial}{\partial R}(\upsilon_i^*\frac{\partial U}{\partial R}) + \frac{1}{R}\frac{\partial}{\partial R}(\upsilon_i^* R\frac{\partial V}{\partial R})$$

$$G = \upsilon_i^*\left[2\{(\frac{\partial U}{\partial X})^2 + (\frac{\partial V}{\partial R})^2 + (\frac{V}{R})^2\} + (\frac{\partial U}{\partial R} + \frac{\partial V}{\partial X})^2 + \{R\frac{\partial}{\partial R}(\frac{W}{R})\}^2 + (\frac{\partial W}{\partial X})^2\right]$$

$$D = 2\upsilon_i^*\left[(\frac{\partial K^{1/2}}{\partial X})^2 + (\frac{\partial K^{1/2}}{\partial R})^2\right]$$

$$E = \frac{2\upsilon_i^*\upsilon_i^*}{\rho}\left[(\frac{\partial^2 U}{\partial X^2})^2 + (\frac{\partial^2 V}{\partial X^2})^2 + (\frac{\partial^2 U}{\partial R^2})^2 + (\frac{\partial^2 U}{\partial R^2})^2\right.$$
$$+ 2\{(\frac{\partial^2 U}{\partial X\partial R})^2 + (\frac{\partial^2 V}{\partial X\partial R})^2\} + \{\frac{\partial}{\partial X}(\frac{V}{R})\}^2 + \{\frac{\partial}{\partial R}(\frac{V}{R})\}^2$$
$$\left. + (\frac{\partial^2 W}{\partial X\partial R})^2 + (\frac{\partial^2 W}{\partial X^2})^2 + \left[\frac{\partial}{\partial R}\{R\frac{\partial}{\partial R}(\frac{W}{R})\}\right]^2 + \left[\frac{\partial}{\partial X}\{R\frac{\partial}{\partial R}(\frac{W}{R})\}\right]^2\right]$$

Table 3 Constants and functions for the low Reynolds number k-ε model [8]

C_1	1.44
σ_k	1.00
σ_ε	1.30
R_t	$k^2/\upsilon_t\varepsilon$
C_2	$1.92\left\{1-0.3\mathrm{Exp}\left(-R_t^2\right)\right\}$
C_μ	$0.09\mathrm{Exp}\left\{\frac{-3.4}{(1+R_t/50)^2}\right\}$

2.5 Boundary Conditions

Following boundary conditions are set to calculate the pressure drop for various cases.

(a) Entrance velocity u_m is constant

(b) At the entrance, turbulence kinetic energy, k, is proportional to u_m^2 and turbulence dissipation rate, ε, is proportional to k^2.

(c) k and ε are zero at the wall.

(d) u and v at the wall are subject to no-slip condition.

(e) Velocity w is an arbitary constant.

In addition, flow boundary condition is applied to exit velocity to match the overall mass balance, and the adiabatic boundary condition is given to other variables (v,w,k and ε) at the exit.

3. NUMERICAL ANALYSIS AND VERIFICATION

Among the available algorithms to calculate the primitive variables in the turbulent flow field, Patanker's SIMPLER Algorithm is selected. Since the low-Reynolds number k-ε turbulence model is selected for this evaluation, finer grid points are taken near the wall. Nonuniform 60*60 grid points are taken with a special care for no grid dependence.

The computation is initialized with 'laminar' computation, and, after certain number of iterations, the turbulent model is applied. This accelerates and stabilizes the convergence. For 'laminar' computation, the velocities are under-relaxed with relaxation factors of 0.7. Later in the 'turbulent' computation, the relaxation factors of 0.4, 0.5, 0.3, 0.3 and 0.5 are used for U, V, K, ε^* and υ_t^* respectively. During each iteration, the convergence occurs only if the difference of flowrate between inflow and outflow in each control volume is less than 10^{-4} and the relative error in flow property at an arbitary point is less than 0.05%.

Also, to evaluate the turbulent flow field in a single cavity for various shaft speeds, this model is compared with Stoff's experiment[1].(see Fig.2)

Fig.2 shows the swirl velocity distribution along the r-direction at the center of the cavity. The current computational results are generally in good agreement with the results of the experiment and is more accurate than those of Stoff's numerical analysis.

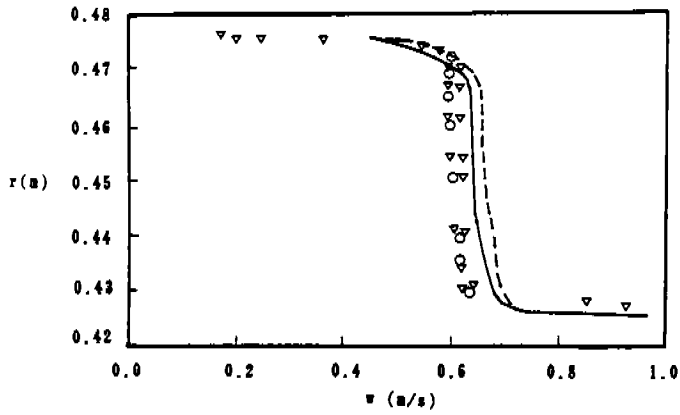

Fig. 2 Radial distribution of the mean circumferential velocity
(a) Stoff 's computation (– – –)
(b) Stoff 's measurement (O , Δ)
(c) Current computation (——)

4. RESULTS AND DISCUSSIONS

The labyrinth seal is widely used in the fluid machinary to minimize the leakage occuring in the region existing pressure difference. Therefore, the leakage may be calculated using pressure boundary condition. However, the leakage is given and the pressure drop is computed alternatively in this study. A single cavity is considered to reduce the computing time and 30℃ water is selected as a working fluid.

The dimensionless bulk pressure drop, which means relative pressure for the left down corner, for the cavity with and without the groove are evaluated for four different Reynolds number (10000, 20000, 30000, and 50000) and three different shaft speeds(0 rpm, 5000 rpm, and 10000 rpm).

Fig.3 shows the velocity vectors and streamlines in the cavity with groove for Re=20,000 and shaft speed 5,000 rpm.

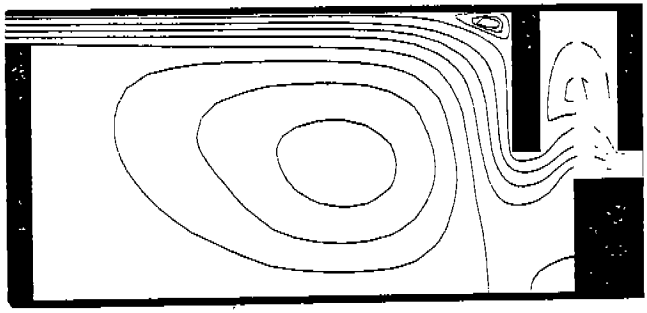

(a) streamline

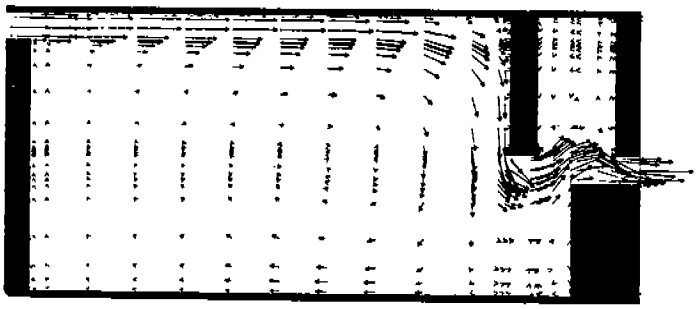

(b) velocity vector

Fig. 3 The streamline and velocity in the cavity with groove
(Re=20,000 and shaft speed=5000rpm)

As shown on Fig.3, a large recirculation zone is formed in the middle of the cavity and small recirculation zones are formed at the front of the step, in the groove and at the down stream corner. The location of the reattachment point is 0.95b and the leakage is expected to decrease if the reattachment point is located futher upstream, thereby increasing the pressure drop.

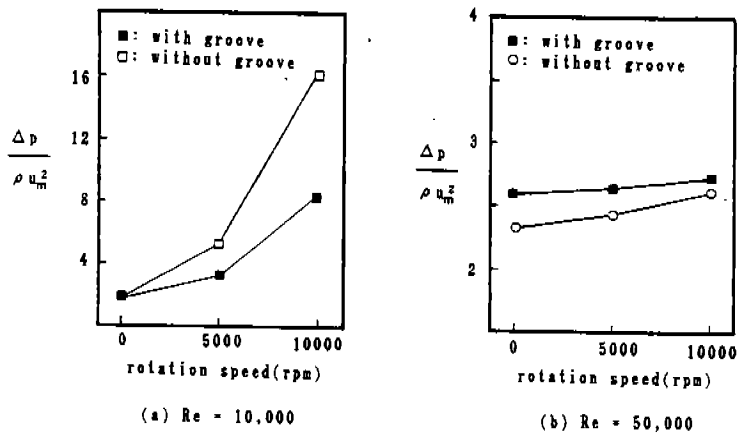

Fig. 4 Pressure drop for shaft speed

Fig.4 shows the pressure drop for various shaft speeds.(Figures for Re=20,000 and 30,000 are not shown here.) It indicates that the pressure drop is very sensitive to the shaft speed at low Reynolds number due to relatively larger circumferential speed than to the axial speed. However, the pressure drop is insensitive to the shaft speed at high Reynolds number. Also, the pressure drops in the cavity with and without groove are nearly the same at low entrance velocity (belower than Re=30,000 or u_m=60m/s) and zero shaft speed. However, as the shaft speed increases, the pressure drop in cavity without groove is greater than that with groove. For Re=30,000 or above, the pressure drop across the cavity with groove, as compared to the cavity without groove, is about 10% greater at zero shaft speed and 4% greater at 10,000 rpm shaft speed. Therefore, the groove works efficiently only at

high Reynolds number.

Fig.5 shows the streamlines in the cavity with groove at Re=10,000 for shaft speed of 0 rpm and 10000 rpm.

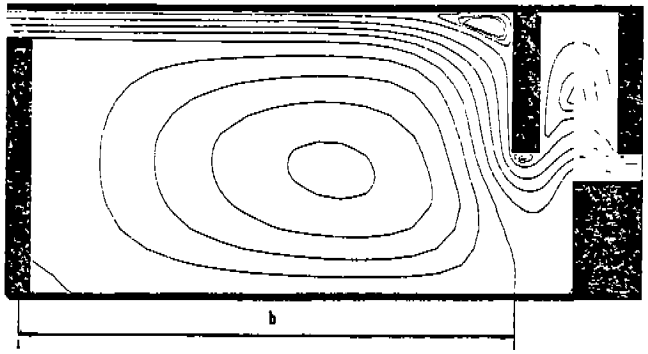

(a) 0 rpm

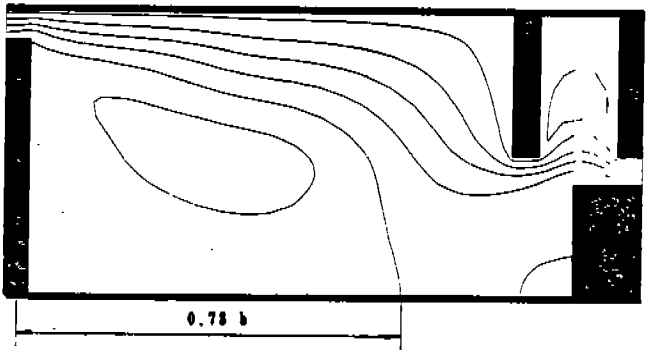

(b) 10,000 rpm

Fig. 5 The streamline of the cavity with groove at Re=10,000

The reattachment point is b for zero shaft speed and 0.78 b for 10000 rpm shaft speed which also shifted to the left. Therefore, the pressure drop increases with the shaft speed.

Fig.6 shows the streamlines in the cavity with groove at Re=50,000 for shaft speed of 0 rpm and 10000 rpm. As explained above, both streamlines are similar to each other regardless of shaft speed due to high main stream velocity at high Reynolds number. Reattachment points are close to each other (0.93 b and 0.92 b). Thus, it is found that the pressure drop is fairly insensitive to the shaft speed at high entrance velocity.

Fig.7 shows the streamslines in the cavity without groove at Re=10,000 for 0 rpm and 10000 rpm.

Comparing Fig.5 and Fig.7, the shape of the streamlines and the location of reattachment points are similar to each other for zero shaft speed and about same pressure drop. However, the reattachment point is shifted slightly to left. This indicates that the pressure drop for the cavity without groove is greater than that with groove. Even though it is not shown here, the streamlines are found to be similar for all three shaft speeds at Re=50,000 except that the

reattachment points for the cavity with groove are relatively shifted to left.

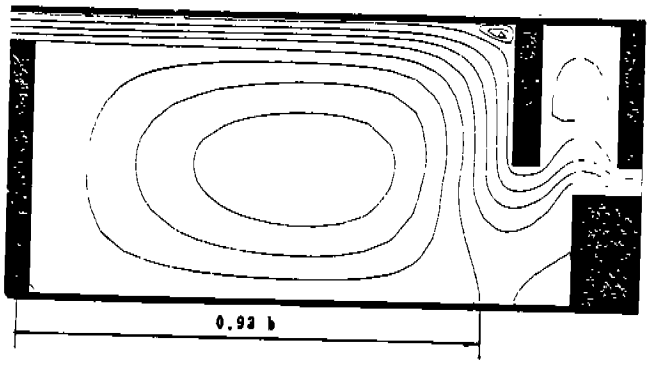

(a) 0 rpm

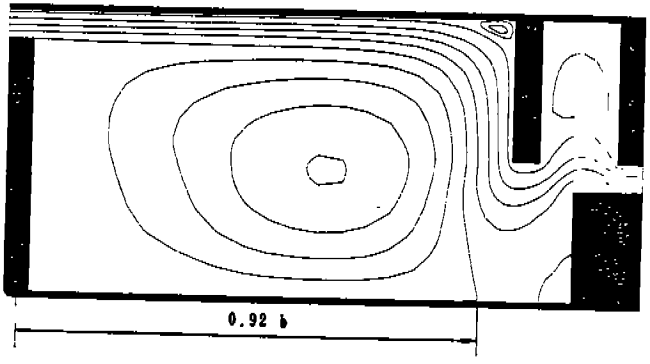

(b) 10,000 rpm

Fig. 6 The streamline of the cavity with groove at Re≈50,000

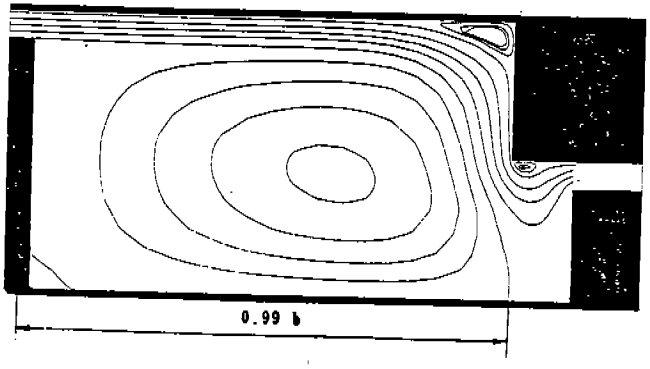

(a) 0 rpm

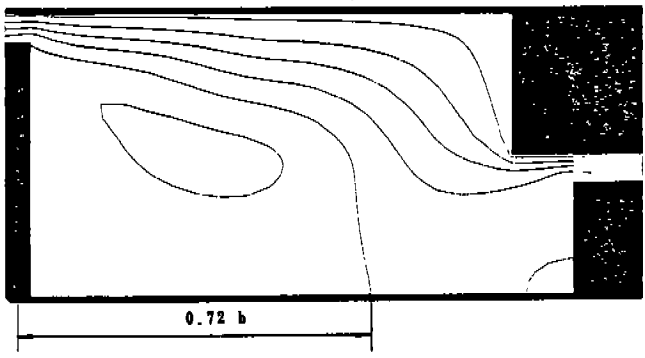

(b) 10,000 rpm

Fig. 7 The streamline of the cavity without groove at Re=10,000

5. CONCLUSIONS

The results of this research can be summarized as :

1. At Re=constant, the pressure drop is proportional to the shaft speed. The slope of pressure drop to the shaft speed is large at low Reynolds number and small at high Reynolds number.

2. The pressure drop is large when the circumferential speed is relatively higher than the axial speed.

3. The pressure drop in the cavity with groove is larger than the case of no groove only at high Reynolds number.

6. REFERENCE

1. H. Stoff, 1980, " Incompressible Flow in a Labyrinth Seal ,"Journal of Fluid Mechanics, Vol. 100, pp. 817-829.
2. D. L. Rhode,J.A.Demko, G. L. Morrison, U. K. Traegner, and S. R. Sobolik,1984, " On the Prediction of Incompressible Flow in Labyrinth Seals ," Trans. ASME, Journal of Fluid Engineering., Vol. 108, pp. 19-25.
3. J. A. Demko, G. L. Morrison, and D. L. Rhode, 1987, " Effect of shaft Rotation on the Incompressible Flow in a Labyrinth Seal ," accepted by the AIAA Journal of Propulsion and Power.
4. D. L. Rhode, G. L. Morrison, S. H. Ko, and S. P. Waughtal, 1987, " Design Improvement of a Pump Wear Ring Labyrinth Seal ," Final Report Contract for Nas 8-36161.
5. L. Dodge, 1963, " Labyrinth Shaft Seals ," Product Engineering Vol. 34, No. 17,pp. 75-79.
6. S. Wittig, K. Jacobsen, U. Schelling, and S. Kim, 1988, " Heat Transfer in Stepped Labyrinth Seals ," Journal of Engineering for Gas Turbines and Power, Vol.110, pp. 63-69.
7. D. L. Rhode, and G.H. Nail, 1988, " Computation of Cavity-By-Cavity Flow Development in Generic Labyrinth Seals ," Turbomachinery Laboratories, Texas A&M Univ. TX77843
8. B. E. Launder and B.I. Sharma, 1974, " Application of the Energy Dissipation Model of Turbulence to the Calculation of Flow Near a Spinning Disc ," Letters in Heat and Mass Transfer, Vol. 1, pp. 131-138.